

Probing quark-lepton correlation in GUTs with high-precision neutrino measurements

Zi-Qiang Chen ^{1,2,3} Gao-Xiang Fang ^{1,2,3} and Ye-Ling Zhou ¹

¹*School of Fundamental Physics and Mathematical Sciences,
Hangzhou Institute for Advanced Study, UCAS, Hangzhou 310024, China*

²*Institute of Theoretical Physics, Chinese Academy of Sciences, Beijing 100190, China*

³*University of Chinese Academy of Sciences, Beijing 100049, China*

(Dated: March 23, 2026)

GUTs unify quarks and leptons into same representations and predict correlations between their masses and mixing. We perform numerical scans in $SO(10)$ GUTs to explore the flavor space with new data of JUNO taken into account. The quark-lepton correlation shows the preference of normal ordering for light neutrino masses, predicts favored region of the CP-violating phase in neutrino oscillations, and classifies GUT models based on their testability in neutrinoless double beta decay experiments. The quark-lepton correlation predicts mass spectrum of right-handed neutrinos, pointing to the energy scale of baryon and lepton number violation and providing sources for baryogenesis. We emphasize that, as high precision measurements of neutrino physics are coming, the quark-lepton correlation will provide increasingly important role in the testability of GUTs, complementary to proton decay measurements.

PACS numbers:

I. INTRODUCTION

Grand Unified Theories (GUTs) do not just unify three gauge interactions of the Standard Model (SM), but also unify Yukawa interactions of quarks and leptons. Of particular interest are the $SO(10)$ GUTs [1] where all SM matter fields are arranged in 16-plets of $SO(10)$ and, as a consequence, all fermion masses and mixing are correlated [2–4]. While the proton decay provides a smoking gun signature of GUTs [5–11], the quark-lepton correlation of masses and mixing might verify the unification of matters via the Yukawa sector. Furthermore, as right-handed neutrinos (RHNs) are embedded into 16-plets, their mass spectrum and Yukawa couplings are predicted by the quark-lepton correlation, and successful leptogenesis becomes testable in the seesaw framework.

The historical intertwining between neutrino measurements and GUTs dates back to the early 1980's, when the first generation experiments represented by IMB and KamiokaNDE were operated (see in review [12]). Current best limits on proton decay are set by the second generation singularly comprised of Super-Kamiokande [13, 14]. The latter is most famous for its observation of atmospheric neutrino oscillation in 1998 [15].

JUNO [16], Hyper-K [17] and DUNE [18] are three main large-scale neutrino oscillation measurements in this stage. They will continue on proton decay measurements to test GUTs and push sensitivities by one order of magnitude. In the meantime, the most important goals are the determination of the neutrino mass ordering (normal $m_1 < m_2 < m_3$ or inverted $m_3 < m_1 < m_2$) and measurement of the Dirac-type CP-violating phase δ . The octant of θ_{23} (1st octant $0 < \theta_{23} < 45^\circ$) and (2nd octant $45^\circ < \theta_{23} < 90^\circ$) will be confirmed and measurements of other oscillation parameters with precision up to sub-percent level will be carried out.

JUNO released the first data on the measurement of $\sin^2 \theta_{12}$ and Δm_{21}^2 after two months of running, with pre-

cision improved by a factor of 1.6 relative to the combination of all previous measurements [19]. In the stage of high-precision neutrino data, the quark-lepton correlation provides a tool of increasing significance to test GUTs complementary to proton decay. We will use the quark-lepton correlation in $SO(10)$ GUTs as a criterion to explore the preferred distribution of unresolved physical observables, including neutrino mass ordering, the favored range of the Dirac CP-violating phase, and effective mass in neutrinoless double-beta ($0\nu\beta\beta$) decay. These quantities will all be tested in the precision era of neutrino physics. In addition, the quark-lepton correlation predicts right-handed neutrino mass spectrum, which touches to the $B - L$ breaking scale and provides sources for baryon-antibaryon asymmetry in the observed Universe. The rest of this paper is organized as follows. Section II gives an overview on Yukawa couplings in $SO(10)$ GUTs. Numerical analysis based on quark-lepton correlation is performed in Section III. We summarize and discuss our results in Section IV.

II. OVERVIEW ON YUKAWAS

In $SO(10)$ GUTs, all matter fields, including SM fermions (quarks, charged leptons and the left-handed neutrinos) and right-handed neutrinos, of the same generation are arranged into a single 16-dim chiral representation 16_F . Following the decomposition $16 \times 16 = 10 + 120 + 126$, a “full” Higgs content for Yukawa couplings could be 10_H , 120_H and $\overline{126}_H$. Yukawa interactions in $SO(10)$ GUTs are generically given by

$$16_F [Y_{10} 10_H + Y_{126} \overline{126}_H + Y_{120} 120_H] 16_F + \text{h.c.} \quad (1)$$

Here, 10_H , 120_H can be either real or complex, which will be denoted with superscripts \mathbb{R} and \mathbb{C} , respectively, and $\overline{126}_H$ is always complex following its representation property. Complexifying the Higgs induces couplings with the conjugates $(10_H^{\mathbb{C}})^*$ and $(120_H^{\mathbb{C}})^*$. They can be forbid-

den by imposing the global Peccei-Quinn (PQ) symmetry $U(1)_{\text{PQ}}$ [20, 21], which gives a compelling explanation of the strong CP problem [22]. Fermions and Higgses under $U(1)_{\text{PQ}}$ transform as

$$\begin{aligned} 16_F &\rightarrow e^{i\alpha} 16_F, & 10_H^{\text{C}} &\rightarrow e^{-2i\alpha} 10_H^{\text{C}}, \\ \overline{126}_H^{\text{C}} &\rightarrow e^{-2i\alpha} \overline{126}_H^{\text{C}}, & 120_H^{\text{C}} &\rightarrow e^{-2i\alpha} 120_H^{\text{C}}. \end{aligned} \quad (2)$$

Accounting for 3 flavors of fermions, all Yukawa couplings are 3×3 matrices, and in particular, Y_{10} , Y_{126} are symmetric and Y_{120} is anti-symmetric in the flavor basis.

Following the symmetry breaking from GUTs to the SM, these Higgs fields are eventually decomposed to eight electroweak doublets in total,

$$h_i = \{\tilde{h}_{10}^u, h_{10}^d, \tilde{h}_{126}^u, h_{126}^d, \tilde{h}_{120_1}^u, h_{120_1}^d, \tilde{h}_{120_{15}}^u, h_{120_{15}}^d\}, \quad (3)$$

where $\tilde{h}_{10}^u = i\sigma_2(h_{10}^u)^*$ [23]. These field decompositions introduce particles beyond the SM spectrum and the SM Higgs is regarded as the lightest and massless one of their eigenstates. Below the GUT scale, it is convenient to write out Yukawa coupling matrices for quarks and leptons

$$\begin{aligned} Y_u &= c_{10}^u Y_{10} + c_{126}^u Y_{126} + (c_{120_1}^u + c_{120_{15}}^u) Y_{120}, \\ Y_d &= c_{10}^d Y_{10} + c_{126}^d Y_{126} + (c_{120_1}^d + c_{120_{15}}^d) Y_{120}, \\ Y_e &= c_{10}^d Y_{10} - 3c_{126}^d Y_{126} + (c_{120_1}^d - 3c_{120_{15}}^d) Y_{120}, \\ Y_\nu &= c_{10}^u Y_{10} - 3c_{126}^u Y_{126} + (c_{120_1}^u - 3c_{120_{15}}^u) Y_{120}. \end{aligned} \quad (4)$$

And mass matrices for quarks and leptons as well as the Dirac mass matrix for neutrinos are generated after the electroweak symmetry breaking, $M_f = Y_f v$ with $f = u, d, e, \nu$ and $v = 174$ GeV. The $\overline{126}_H$ Higgs contains scalars of the charge $B - L = 2$. They are essential to generate light neutrino masses via seesaw mechanism,

$$\begin{aligned} M_R &= v_S Y_{126}, \\ M_\nu &= -Y_\nu M_R^{-1} Y_\nu^T v^2, \end{aligned} \quad (5)$$

where v_S is the scalar VEV and we have assumed type-I seesaw dominance. Since all SM fermion mass matrices M_u, M_d, M_e and M_ν are correlated, it is obvious that masses of quarks and leptons, and the consequent flavor mixing (i.e., Cabibbo-Kobayashi-Maskawa (CKM) and Pontecorvo-Maki-Nakagawa-Sakata (PMNS) mixing), are all correlated via the above formulas.

While the general Yukawa couplings in Eq. (1) leaves plenty of room to fit data of fermion masses and mixing, economical models have been considered to reduce the number of free parameters. We discuss the economical and realistic Higgs content to be included in this work. First, one single Higgs multiplet (either 10_H , $\overline{126}_H$ or 120_H) is not enough, since it fails to generate fermion masses and no flavor mixing in either quark or lepton sector. To explain tiny masses for light neutrinos, $\overline{126}_H$ must be included since it is the only Higgs involving a

TABLE I: A complete list of possible combinations of Higgs content in renormalizable $SO(10)$ GUTs with all fermions arranged in 16_F .

Higgs content	Whether realistic in fitting fermion data
Only one Higgs	No, no flavor mixing
$10_H^{\text{R,C}}, 120_H^{\text{R,C}}$	No, massless light neutrinos
$10_H^{\text{R}}, \overline{126}_H^{\text{C}}$	No, small hierarchy between m_b and m_t
$120_H^{\text{R,C}}, \overline{126}_H^{\text{C}}$	No, inconsistent with mixing data
$10_H^{\text{C}}, \overline{126}_H^{\text{C}}$	Yes, imposing $U(1)_{\text{PQ}}$ leads to M1
$10_H^{\text{R}}, \overline{126}_H^{\text{C}}, 120_H^{\text{R}}$	Yes, assuming SCPV leads to M2
$10_H^{\text{C}}, \overline{126}_H^{\text{C}}, 120_H^{\text{C}}$	Yes, imposing $U(1)_{\text{PQ}} \times Z_2^P$ leads to M3

TABLE II: Representative models to be used in fitting fermion data, their main features and number of free parameters.

Model	Main features	n_{para}
M1	Only Y_{10}, Y_{126}	19
M2	Real Y_{10}, Y_{126}, Y_{120}	19
M3	Hermitian Y_u, Y_d, Y_e, Y_ν	18

SM singlet with charge $B - L = 2$, which is necessary to generate Majorana masses for neutrinos via seesaw mechanism. The minimal extension is by adding a real 10_H^{R} into the theory. However, it cannot explain the large hierarchy between m_b and m_t [21]. On the other hand, the model with $(\overline{126}_H, 120_H)$ is found to be unable to fit all the fermion masses and mixing angles in the three generation case [24, 25]. Then, we are left with a few realistic choices for fitting data, either the minimal Higgs content $(10_H^{\text{C}}, \overline{126}_H^{\text{C}})$ or a complete list $(10_H, \overline{126}_H, 120_H)$. Among them, we will focus on three compelling models.

- **M1** – $(10_H^{\text{C}}, \overline{126}_H^{\text{C}})$ with $U(1)_{\text{PQ}}$.
This one introduces the minimal Higgs contents among the realistic models [20]. Imposing $U(1)_{\text{PQ}}$ forbids terms with $(10_H^{\text{C}})^*$ and thus only Y_{10} and Y_{126} are present [26–29]. Without loss of generality, we rotate the flavor basis to keep Y_{126} always real and diagonal. There are $6 \times 2 + 3$ real parameters in Y_{10} and Y_{126} . Additional free parameters includes the relative size and phases among $c_{10,126}^{u,d}$. In total, we have 19 free parameters in the Yukawa sector.
- **M2** – $(10_H^{\text{R}}, \overline{126}_H^{\text{C}}, 120_H^{\text{R}})$ with SCPV.
Complex Yukawas Y_{10}, Y_{126} and Y_{120} leave enough room to fit data. Imposing CP symmetry at high scale reduces the number of free parameters [30–33]. In the basis of diagonal Y_{126} , there are $6 + 3 + 3$ real parameters in Y_{10}, Y_{126}, Y_{120} . The Higgses gain complex VEVs and induce spontaneous CP violation (SCPV). This model introduce also 19 free parameters in the Yukawa sector competitive to **M1**.

- M3 – $(10_H^C, \overline{126}_H^C, 120_H^C)$ with $U(1)_{PQ} \times Z_2^P$.

This model includes a full list of Higgs multiplets [23–25]. $U(1)_{PQ}$ forbids couplings to the complex conjugate of 10_H^C or 120_H^C . Z_2^P represents the left-right parity symmetry $\psi_L \leftrightarrow \psi_R$, which results in Hermitian Yukawa matrices Y_u, Y_d, Y_e, Y_ν [34]. This symmetry is achieved via a CP parity symmetry at high scale, to guarantee real Y_{10}, Y_{126} and Y_{120} . Combining the CP parity with the internal matter parity, i.e., the D parity [35], $\psi_L \leftrightarrow \psi_R^C$, of $SO(10)$ gives rise to Z_2^P . A maximal CP violation is achieved spontaneously if the VEV of 120_H^C is orthogonal to the other two Higgs VEVs in the complex plane, but Z_2^P is left unbroken [36].

We refer to Appendix A for detailed parameterizations of these models.

III. NUMERICAL ANALYSIS

We explore the parameter space allowed by current experiments and discuss their physical predictions for the above three models. The χ^2 function is defined as

$$\chi^2 = \sum_{i=1}^{n_{\text{obs}}} \left(\frac{\mathcal{O}_i - \mathcal{O}_i^{\text{bf}}}{\sigma_{\mathcal{O}_i}} \right)^2, \quad (6)$$

where \mathcal{O}_i is the i -th theoretical prediction, and $\mathcal{O}_i^{\text{bf}}$ is the corresponding i -th experimental best-fit (bf) value, and the $\sigma_{\mathcal{O}_i}$ is the 1σ uncertainty. We take $n_{\text{obs}} = 18$ observables into fitting, including 9 charged fermion masses, 3 angles and 1 phase in the CKM mixing matrix, 2 mass-squared differences and 3 angles in the PMNS mixing matrix. All data are listed in Appendix A. In the neutrino sector, we take NuFIT 6.0 [37] but replace data of Δm_{21}^2 and $\sin^2 \theta_{12}$ (best-fits $\pm 1\sigma$) with the most recent JUNO data,

$$\begin{aligned} \Delta m_{21}^2 &= (7.50 \pm 0.12) \times 10^{-5} \text{eV}^2, \\ \sin^2 \theta_{12}^l &= 0.3092 \pm 0.0087. \end{aligned} \quad (7)$$

NuFIT provides four versions of global data, which we list in Appendix A and denote as N1, N2, I1 and I2, depending on which mass ordering is assumed and whether SK atmospheric data is included. Namely, N1 and N2 represent global fits with and without SK atmospheric data in the normal ordering, and I1 and I2 are those in the inverted ordering. The up-to-date experimental constraint on the Dirac CP-violating phase δ is still weak, and thus is not included in the χ^2 . Instead, we treat δ as a prediction of the model, together with other predictions including the lightest neutrino mass m_{lightest} , the effective masses appearing in β decay m_β , $0\nu\beta\beta$ decay $m_{\beta\beta}$, and right-handed neutrino masses M_1, M_2, M_3 (from lightest to heaviest).

We perform numerical scan for all three models M1, M2, M3 with four versions of data respectively accounted. Same procedures of scan are performed in all cases. All viable points for $\chi^2/n_{\text{obs}} < 10$ in these models are presented in Appendix A, in Figs. 3 and 4 for normal and

inverted ordering, respectively. Representative benchmarks in these models are presented in Appendix B.

We first report results on the prediction of neutrino mass ordering. In model M1, no viable points in the inverted ordering are found to fit data in our scan. In models M2 and M3, although both normal and inverted ordering can fit data, the former case is highly favored due to its efficiency in the scan. Scan efficiencies of models in fitting both mass ordering are compared in Fig. 1.

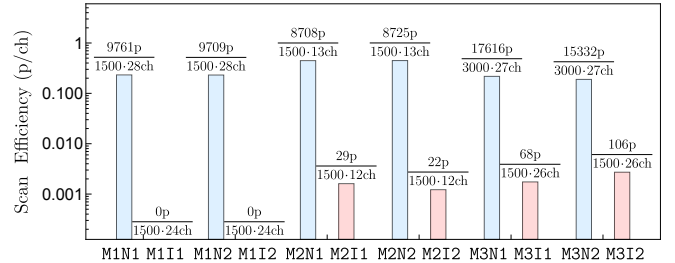


FIG. 1: Viable points (p) per core hour (ch) obtained in M1, M2 and M3 with $\chi^2/n_{\text{obs}} < 10$ in each scan.

Below we will mainly focus on the normal mass ordering. Note that data N1 and N2 prefer θ_{23} in the 1st octant ($\theta_{23} < 45^\circ$) and 2nd octant ($\theta_{23} > 45^\circ$), respectively. Thus, we can further check the preference of the θ_{23} octant in models. Given points in Fig. 3, we count points in certain intervals normalized by the corresponding weight $e^{-\chi^2/2}$ and obtain the preferred regimes of observables in models. General results on predictions of θ_{23} , δ and RHN masses are shown in Fig. 2 and summarized as follows. By taking data of θ_{23} in both octants, we find a slight preference on the 1st octant in M2, but no significant preference of the octant in M1 and M3. Distributions of δ are different in three models. δ is mainly distributed in the region $[-70^\circ, +70^\circ]$ in M2, extended to $[-90^\circ, +90^\circ]$ in M3 and spanned into most of the parameter space in M1.

We discuss the predictions of RHN mass spectrum and potentially consequent phenomenon. These models predict very different mass spectrums for RHNs. We have confirmed the large hierarchy of RHN masses in M2 which has been studied in [32], where the lightest one can be as small as 10^4 GeV and the heaviest one can reach 10^{15} GeV. However, more points show the lightest mass M_1 span in the interval $[4 \cdot 10^4, 3 \cdot 10^7]$ GeV. This regime has not been discovered before. Both M1 and M3 show much smaller hierarchies. M1 gives a clear prediction on M_1 around $[10^9, 10^{10}]$ GeV and the highest one $M_3 \sim [10^{12}, 10^{13}]$ GeV, where most points give $M_1/M_3 \sim 10^{-3}$. Predictions in M3 are more diverse, although a lot of them gives $M_1 \sim 10^{10}$ GeV and $M_3 \sim 10^{13}$ GeV. This result is consistent with former results [23], but we have found more parameter space.

A clear prediction of RHN mass spectrum serves as the basis for numerous interesting research avenues. We briefly address them below. RHNs provide an explana-

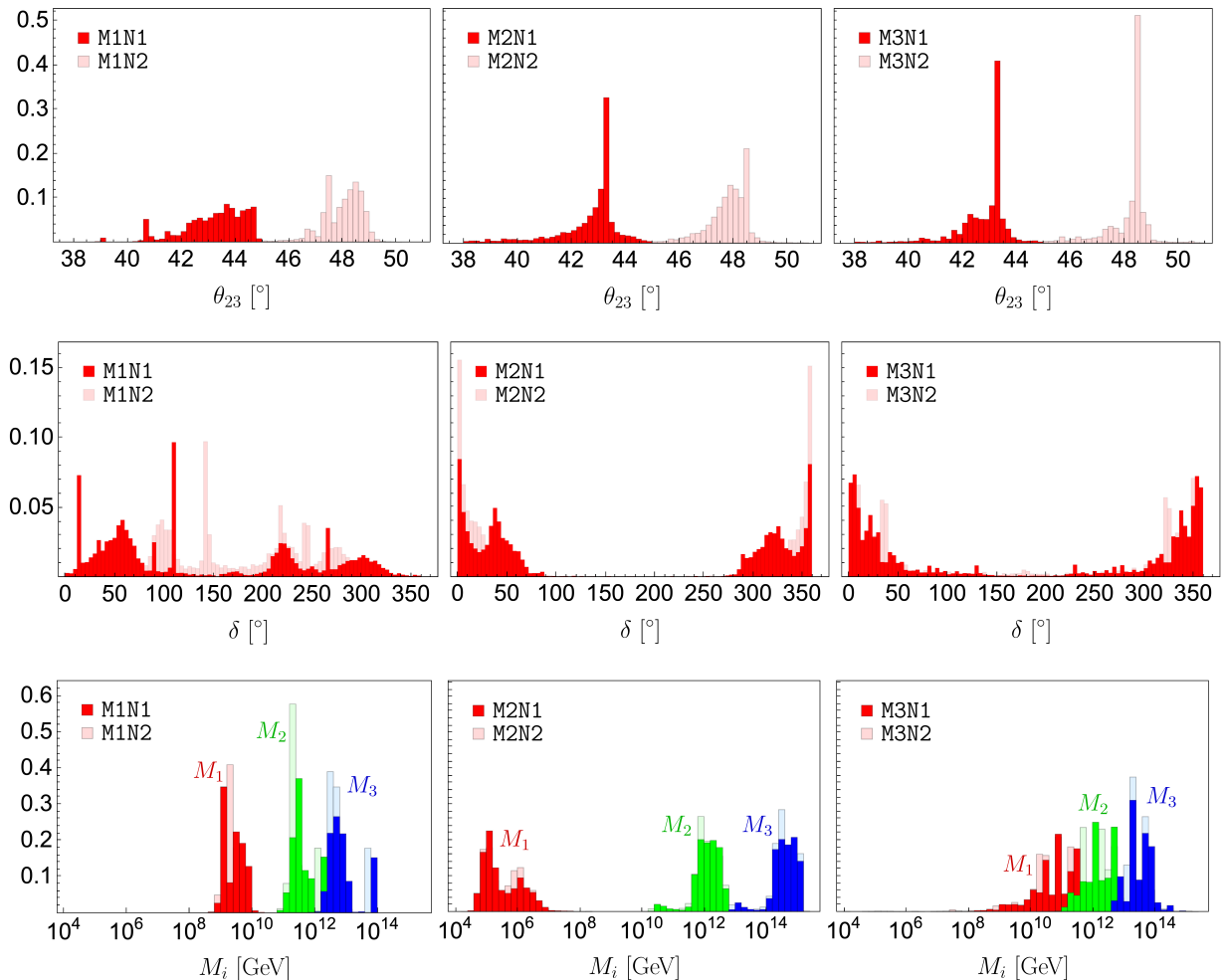


FIG. 2: Predicted distributions of some observables of models M1, M2 and M3 in the normal order in fitting data N1 and N2 in the normal ordering. RHN masses M_1 , M_2 and M_3 are marked in red, green and blue, respectively in the bottom panel.

tion of baryon-antibaryon asymmetry via the mechanism of leptogenesis. This is quantitatively calculated via the quark-lepton correlation in $SO(10)$ GUTs. A successful thermal leptogenesis requires M_1 heavier than 10^9 GeV [38], which applies for most points in M1 and M3. However, this condition is not satisfied in M2, and inspires alternative scenarios, e.g., N_2 leptogenesis [39], might succeed

IV. CONCLUSION AND DISCUSSIONS

GUTs unify quarks and leptons and predict correlation between their masses and mixing. We emphasize that the quark-lepton correlation can play increasingly important role to test GUTs with the help of high-precision neutrino measurements in the coming decade.

We begin with a brief review on the fermion masses and mixing in $SO(10)$ GUTs. Then we take three representative GUT models as examples to explore the flavor space consistent with experimental data. In particular, the most recent JUNO data has been taken into account.

in some parameter space [33]. In a perturbative theory, all RHN masses should not be heavier than the $B - L$ energy scale. That means this scale should be heavier than $M_3 \sim 10^{13}$ GeV for most points in M1 and M3. In M2, the heaviest RHN can be as heavy as 10^{15} GeV. A $B - L$ scale above this value requires special RG effects to be included in the gauge unification.

The quark-lepton correlation shows the preferred distribution of unresolved physical observables. We argue that inverted ordering for neutrino masses are disfavored in $SO(10)$ GUTs. The Dirac CP-violating phase and neutrinoless double beta decay are predicted differently in these models. Forthcoming measurements will be able to classify GUT models. These quantities will all be tested in the precision era of neutrino physics. The quark-lepton correlation further predicts right-handed neutrino masses. Different hierarchies of their mass scales point to different scenarios of leptogenesis in explanation of

matter-antimatter asymmetry in our observed universe. The restrictions on the $B - L$ scale touches to the gauge unification in GUTs. We suggest to use the quark-lepton correlation as a tool to evaluate GUTs in the precision era of neutrino physics.

Acknowledgments

This work was supported by Zhejiang Provincial Natural Science Foundation of China (No. LDQ24A050002) and National Natural Science Foundation of China (NSFC) (Nos. 12535007 and 12547104).

A. Details of fitting procedure

After GUT symmetry breaking, $10_H, \overline{126}_H, 120_H$ are decomposed to a series of electroweak doublets of the SM gauge symmetry, denoted in Eq. (3). They mix and the lightest massless one matches to the SM Higgs. After the SM Higgs gains the VEV v , triggering the electroweak symmetry breaking, the SM fermions obtain masses. We parameterize VEVs of electroweak doublets as

$$\begin{aligned} & \{\langle h_{10}^u \rangle, \langle h_{10}^d \rangle, \langle h_{120_1}^u \rangle, \langle h_{120_1}^d \rangle\} \\ &= \{c_{10}^u, c_{10}^d, c_{120_1}^u, c_{120_1}^d\} \times \frac{v}{\sqrt{2}}; \\ & \{\langle h_{126}^u \rangle, \langle h_{126}^d \rangle, \langle h_{120_{15}}^u \rangle, \langle h_{120_{15}}^d \rangle\} \\ &= \{c_{126}^u, c_{126}^d, c_{120_{15}}^u, c_{120_{15}}^d\} \times \sqrt{\frac{3}{2}}v, \end{aligned} \quad (A1)$$

where all $c_{\text{rep}}^{u,d}$ are dimensionless and complex parameters, and overall factors in front of v are induced by representation decomposition in group theory, which are irrelevant to our fit. We further parameterize $c_{\text{rep}}^{u,d}$ by removing unphysical parameters. Without loss of generality, c_{126}^u can be rotated to be real, and remaining coefficients are generally complex. Concretely we write

$$\begin{aligned} c_{10}^u &= |c_{10}^u|e^{i\alpha}, \quad c_{10}^d = |c_{10}^d|e^{i\beta}, \\ c_{126}^u &= |c_{126}^u|, \quad c_{126}^d = |c_{126}^d|e^{i\omega}, \quad v_S = |v_S|, \\ c_{120_1}^u + c_{120_{15}}^u &= |c_{120_1}^u + c_{120_{15}}^u|e^{i\lambda}, \\ c_{120_1}^d + c_{120_{15}}^d &= |c_{120_1}^d + c_{120_{15}}^d|e^{i\rho}, \\ c_{120_1}^u - 3c_{120_{15}}^u &= |c_{120_1}^u - 3c_{120_{15}}^u|e^{i\gamma}, \\ c_{120_1}^d - 3c_{120_{15}}^d &= |c_{120_1}^d - 3c_{120_{15}}^d|e^{i\eta}, \end{aligned} \quad (A2)$$

Moreover, the SM singlet scalar VEV v_S can also taken to be real. Therefore, Yukawa matrices and parameters are written as

$$\begin{aligned} D &= |c_{126}^u|Y_{126}, \quad S = |c_{10}^u|Y_{10}, \quad A = |c_{120_1}^u + c_{120_{15}}^u|Y_{120}, \\ v_R &= \frac{|v_S|}{|c_{126}^u|}, \quad r_1 = \frac{|c_{126}^d|}{|c_{126}^u|}, \quad r_2 = \frac{|c_{10}^d|}{|c_{10}^u|}, \quad r_3 = \frac{|c_{120_1}^d + c_{120_{15}}^d|}{|c_{120_1}^u + c_{120_{15}}^u|}, \\ r_4 &= \frac{|c_{120_1}^d - 3c_{120_{15}}^d|}{|c_{120_1}^u + c_{120_{15}}^u|}, \quad r_5 = \frac{|c_{120_1}^u - 3c_{120_{15}}^u|}{|c_{120_1}^u + c_{120_{15}}^u|}. \end{aligned} \quad (A3)$$

With the above preparation, three models in this paper can be reparameterized, as below.

$$\begin{aligned} \text{M1, } & 10_H^{\text{C}} + \overline{126}_H^{\text{C}} \text{ with } U(1)_{\text{PQ}} \\ & Y_u = S + D, \end{aligned}$$

$$\begin{aligned} Y_d &= r_2 S + e^{i\omega} r_1 D, \\ Y_e &= r_2 S - 3e^{i\omega} r_1 D, \\ Y_\nu &= S - 3D, \\ M_R &= v_R D, \end{aligned} \quad (A4)$$

where the phase of c_{10}^u , can be absorbed into S and an overall phase between S terms and D terms in Y_d is unphysical and has been ignored. Here we follow the convention in Ref. [40], with a basis where the symmetric matrix D is real and diagonal, whence S becomes a general complex symmetric matrix. r_1, r_2, v_R are real parameters and ω is a phase.

$$\text{M2, } 10_H^{\text{R}} + \overline{126}_H^{\text{C}} + 120_H^{\text{R}} \text{ with SCPV}$$

As $10_H, 120_H$ are real fields, VEVs of Higgs doublets in these two fields have relations $v_{10}^d = v_{10}^{u*}, v_{120_1}^d + v_{120_{15}}^d = v_{120_1}^{u*} + v_{120_{15}}^{u*}, v_{120_1}^d - 3v_{120_{15}}^d = v_{120_1}^{u*} - 3v_{120_{15}}^{u*}$. Next, we follow the convention in Ref. [33], the Dirac mass matrices of fermions can be reparameterized as

$$\begin{aligned} Y_u &= e^{i\alpha} S + D + e^{i\lambda} A, \\ Y_d &= e^{-i\alpha} S + e^{i\omega} r_1 D + e^{-i\lambda} A, \\ Y_e &= e^{-i\alpha} S - 3e^{i\omega} r_1 D + e^{-i\gamma} r_4 A, \\ Y_\nu &= e^{i\alpha} S - 3D + e^{i\gamma} r_4 A, \\ M_R &= v_R D. \end{aligned} \quad (A5)$$

Due to the CP symmetry, Y_{10}, Y_{126}, Y_{120} are all real, equivalently S, D, A are real matrices and M_R is a real symmetric matrix. Here, we work in a basis where D is diagonal and positive. S is real symmetric and A is real antisymmetric. r_1, r_4, v_R are real parameters and $\alpha, \lambda, \gamma, \omega$ are phases.

$$\text{M3, } 10_H^{\text{C}} + \overline{126}_H^{\text{C}} + 120_H^{\text{C}} \text{ with } U(1)_{\text{PQ}} \times Z_2^P$$

The Dirac mass matrices of fermions are reparameterized as

$$\begin{aligned} Y_u &= S + D + iA, \\ Y_d &= r_2 S + r_1 D + ir_3 A, \\ Y_e &= r_2 S - 3r_1 D + ir_4 A, \\ Y_\nu &= S - 3D + ir_5 A, \\ M_R &= v_R D. \end{aligned} \quad (A6)$$

We follow the convention in Ref. [23], as CP invariance above the GUT scale and spontaneous CP violation (SCPV) below the GUT scale, S, D, A are real matrices, resulting Y_u, Y_d, Y_e, Y_ν are Hermitian matrices and M_R is a real symmetric matrix. Consistent with previous models, we still choose a basis where D is diagonal and positive, S is real symmetric and A is real antisymmetric. $r_1, r_2, r_3, r_4, r_5, v_R$ are real parameters.

Parameters of these models are summarized in Table III.

TABLE III: Parameters counting in three models.

Label	Free parameters
M1 ($n_{\text{para}} = 19$)	$\{r_1, r_2\} \in (-10, 10)$, $m_0 \in (0, 1)$ eV, $\omega \in [0, 2\pi)$, $D : \{D_{11}, D_{22}, D_{33}\} \in (0, 1)$, $S : \{S_{11}e^{is_1}, S_{12}e^{is_2}, S_{13}e^{is_3}, S_{22}e^{is_4}, S_{23}e^{is_5}, S_{33}e^{is_6}\} \in (-10, 10)e^{i[0, 2\pi)}$
M2 ($n_{\text{para}} = 19$)	$\{r_1, r_4\} \in (-10, 10)$, $m_0 \in (0, 1)$ eV, $\{\alpha, \lambda, \gamma, \omega\} \in [0, 2\pi)$, $D : \{D_{11}, D_{22}, D_{33}\} \in (0, 1)$, $S : \{S_{11}, S_{12}, S_{13}, S_{22}, S_{23}, S_{33}\} \in (-10, 10)$, $A : \{A_{12}, A_{13}, A_{23}\} \in (-10, 10)$
M3 ($n_{\text{para}} = 18$)	$\{r_1, r_2, r_3, r_4, r_5\} \in (-10, 10)$, $m_0 \in (0, 1)$ eV, $D : \{D_{11}, D_{22}, D_{33}\} \in (0, 1)$, $S : \{S_{11}, S_{12}, S_{13}, S_{22}, S_{23}, S_{33}\} \in (-10, 10)$, $A : \{A_{12}, A_{13}, A_{23}\} \in (-10, 10)$

Data ($\text{bf} \pm 1\sigma$) for quark Yukawas and mixing parameters, as well as charged lepton Yukawas, are listed below, taken from [30] with RG effect running up to $M_{\text{GUT}} = 2 \times 10^{16}$ GeV.

$$\begin{aligned}
y_u &= (2.54 \pm 0.86) \cdot 10^{-6}, & y_d &= (6.56 \pm 0.65) \cdot 10^{-6}, \\
y_c &= (1.37 \pm 0.04) \cdot 10^{-3}, & y_s &= (1.24 \pm 0.06) \cdot 10^{-4}, \\
y_t &= (0.428 \pm 0.003), & y_b &= (5.7 \pm 0.005) \cdot 10^{-3}, \\
\theta_{12}^q &= (0.227 \pm 0.0006), & \theta_{13}^q &= (4.202 \pm 0.13) \cdot 10^{-3}, \\
\theta_{23}^q &= (4.858 \pm 0.06) \cdot 10^{-2}, & \delta^q &= (1.207 \pm 0.054);
\end{aligned} \tag{A7}$$

$$\begin{aligned}
y_e &= (2.703 \pm 0.027) \cdot 10^{-6}, & y_\mu &= (5.707 \pm 0.057) \cdot 10^{-4}, \\
y_\tau &= (9.702 \pm 0.0097) \cdot 10^{-3},
\end{aligned} \tag{A8}$$

For charged lepton Yukawas, we have quoted error to be 1% uncertainty in their masses to relax the difficulty induced by the tiny experimental errors of charged lepton masses [32]. Oscillation data except Δm_{21}^2 and $\sin^2 \theta_{12}$ in the normal ordering are taken from NuFIT 6.0 [37]. We apply following four versions of data: normal ordering for IC24 with SK atmospheric data (denoted as N1),

$$\begin{aligned}
\sin^2 \theta_{23} &= 0.470 \pm 0.015, & \sin^2 \theta_{13} &= 0.02215 \pm 0.00057 \\
\Delta m_{31}^2 &= (2.513 \pm 0.020) \times 10^{-3} \text{eV}^2;
\end{aligned} \tag{A9}$$

normal ordering for IC19 without SK atmospheric data (N2),

$$\begin{aligned}
\sin^2 \theta_{23} &= 0.561 \pm 0.014, & \sin^2 \theta_{13} &= 0.02195 \pm 0.00056, \\
\Delta m_{31}^2 &= (2.534 \pm 0.024) \times 10^{-3} \text{eV}^2;
\end{aligned} \tag{A10}$$

inverted ordering with SK atmospheric data (I1),

$$\begin{aligned}
\sin^2 \theta_{23} &= 0.550 \pm 0.014, & \sin^2 \theta_{13} &= 0.02231 \pm 0.00056 \\
\Delta m_{32}^2 &= (-2.484 \pm 0.020) \times 10^{-3} \text{eV}^2;
\end{aligned} \tag{A11}$$

and inverted ordering without SK atmospheric data (I2),

$$\begin{aligned}
\sin^2 \theta_{23} &= 0.562 \pm 0.014, & \sin^2 \theta_{13} &= 0.02224 \pm 0.00057 \\
\Delta m_{32}^2 &= (-2.510 \pm 0.025) \times 10^{-3} \text{eV}^2.
\end{aligned} \tag{A12}$$

In the inverted ordering, both I1 and I2 support θ_{23} in the 2nd octant. NuFIT data of $\sin^2 \theta_{12}$ and Δm_{21}^2 in inverted ordering keep the same,

$$\begin{aligned}
\sin^2 \theta_{12} &= 0.308 \pm 0.012, \\
\Delta m_{21}^2 &= (7.49 \pm 0.19) \times 10^{-5} \text{eV}^2,
\end{aligned} \tag{A13}$$

In all of our scans, the same procedure is performed as below.

1. Firstly, we begin with 15000 randomly generated points whose parameters x_i^0 (where i runs over all free parameters of each model) are sampled within their defined region shown in Tab. III. From these parameters, we obtain light neutrino mass matrix via seesaw formula and Dirac mass matrices. The initial value of χ^2 is usually very large, of order 10^8 .
2. Then, we minimize χ^2 using the differential evolution (DE) algorithm from the SciPy library. The DE algorithm optimizes all points simultaneously. The configuration uses 15,000 independent chains running in parallel via MPI, with each chain maintaining a population of 15 points. The `best1bin` mutation strategy ($F = 0.7$) is applied for up to 50000 generations.
3. Finally, we truncate points with $\chi^2/n_{\text{obs}} < 10$ for each model.

Our scan is performed on the HIAS cluster with 3000 CPU cores available. Code and derived points of all three models are released in GitHub. We further show these points in Fig. 3 in the normal ordering and Fig. 4 in the inverted ordering.

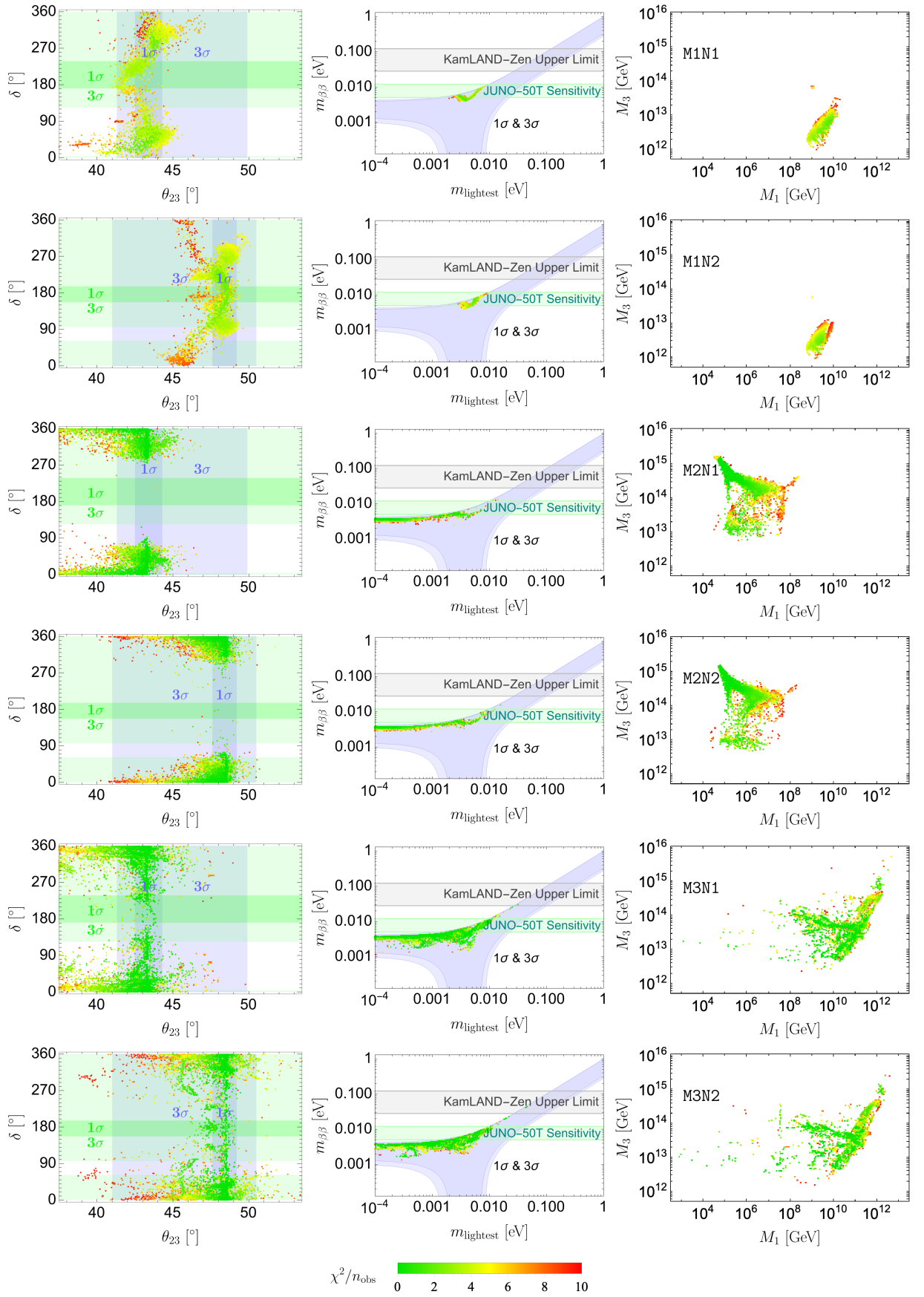


FIG. 3: Predictions of models M1, M2 and M3 for $\chi^2/n_{\text{obs}} < 10$ in fitting data N1 and N2 in the normal ordering.

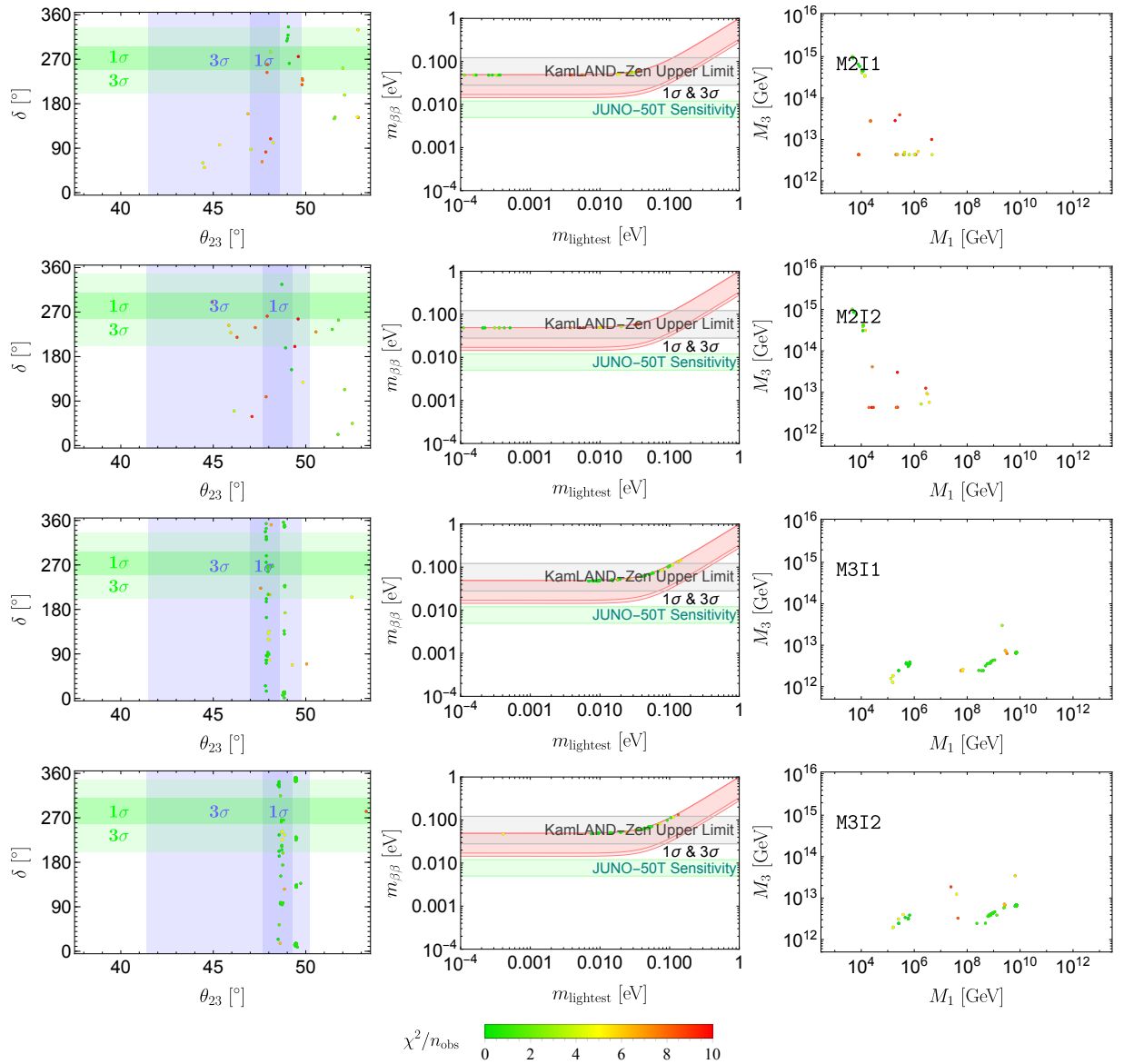


FIG. 4: Predictions of models M2 and M3 for $\chi^2/n_{\text{obs}} < 10$ in fitting data I1 and I2 in the inverted ordering. M1 is not shown since no viable points found in the inverted ordering.

In the normal ordering of light neutrino masses, using model M1 to fit data N1 (M1N1) or M1 to fit N2 (M1N2) complete their scan using 1500 CPU cores in 28 hours and minimize the χ^2 value to $\chi_{\text{min}}^2/n_{\text{obs}} = 1.54, 1.71$. M2N1 and M2N2 complete scans with 1500 CPU cores in 13 hours and get $\chi_{\text{min}}^2/n_{\text{obs}} = 3.34 \times 10^{-6}, 7.60 \times 10^{-6}$. M3N1 and M3N2 complete scans using 3000 CPU cores in 27 hours and get final $\chi_{\text{min}}^2/n_{\text{obs}} = 3.41 \times 10^{-7}, 3.19 \times 10^{-7}$.

In the inverted ordering, we fit I1 and I2 in model M1 with 1500 CPU cores in 24 hours, and obtain $\chi_{\text{min}}^2/n_{\text{obs}} = 147.41$ and 147.64 , respectively, thus, no viable point for model M1 found in the inverted ordering. In model M2, M2I1 and M2I2 complete scans with 1500 CPU cores in 12

hours and obtain $\chi_{\text{min}}^2/n_{\text{obs}} = 0.205$ and 0.00721 , respectively. M3I1 and M3I2 complete scans using 1500 CPU cores in 26 hours and obtain $\chi_{\text{min}}^2/n_{\text{obs}} = 0.0680$ and 0.598 , respectively.

We comment on the prediction of light neutrino masses which are not discussed in the maintext. In the normal ordering, the lightest neutrino mass m_1 is predicted around the region $[0.002, 0.01]$ eV in M1, $(0, 0.015]$ eV in M2 and mainly distributed in $(0, 0.02]$ eV in M3. $m_{\beta\beta}$ in M1 is predicted in a narrow regime $[0.004, 0.01]$ eV, which can be tested in the future $0\nu\beta\beta$ experiments. M2 prefers a smaller value, mainly in the region $[0.003, 0.006]$ eV, below the experimental sensitivity. The predicted region in

M3 overlaps with both models. In the inverted ordering, the lightest neutrino mass m_3 is smaller than 0.02 eV and $0\nu\beta\beta$ mass $m_{\beta\beta} \gtrsim 0.05$ eV in our limited data points.

B. Benchmark studies

We show benchmark points of M1, M2 and M3 in Tab. IV and V with four versions of data N1, N2, I1 and N2 all taken into account. In models M2 and M3, as di-

verse mass hierarchies for RHNs are predicted, we show a few distinguishable benchmarks in these models. For example, very large hierarchy $(M_1, M_2, M_3) = (9.95 \cdot 10^4, 2.14 \cdot 10^{12}, 7.51 \cdot 10^{14})$ GeV is predicted in M2N1B1, which is consistent with the ansatz assumed in [32], relatively smaller hierarchy $(M_1, M_2, M_3) = (7.36 \cdot 10^6, 6.96 \cdot 10^{10}, 2.29 \cdot 10^{13})$ GeV is also found in M2N1B2 in our scan.

TABLE IV: Benchmark fit values and predictions in 3 models in the normal ordering. Each benchmark is named, e.g., M1N1B1: benchmark 1 of M1 in fitting data N1. $\Delta m_{3l}^2 = \Delta m_{31}^2 > 0$ and $m_l = m_1$ denote the lightest neutrino mass. We distinguish different benchmarks, e.g., M1N1B1 vs M1N1B2, due to the different hierarchies of RHN masses are predicted when fitting the same data in the same model.

Physical Quantity	M1		M2				M3			
	M1N1B1	M1N2B1	M2N1B1	M2N1B2	M2N2B1	M2N2B2	M3N1B1	M3N1B2	M3N2B1	M3N2B2
$y_u/10^{-6}$	2.65	2.75	2.55	3.07	2.53	4.85	0.637	2.54	0.744	2.54
$y_c/10^{-3}$	1.40	1.39	1.37	1.35	1.37	1.37	1.37	1.37	1.37	1.37
y_t	0.429	0.427	0.428	0.429	0.428	0.430	0.428	0.428	0.428	0.428
$y_d/10^{-6}$	3.87	3.13	6.56	7.29	6.56	7.14	5.28	6.56	5.28	6.56
$y_s/10^{-4}$	1.37	1.32	1.24	1.17	1.24	1.11	1.24	1.24	1.25	1.24
$y_b/10^{-2}$	0.571	0.571	0.570	0.570	0.570	0.568	0.569	0.570	0.569	0.570
$y_e/10^{-6}$	2.69604	2.70309	2.70346	2.70190	2.70339	2.70629	2.70318	2.70346	2.70345	2.70341
$y_\mu/10^{-4}$	5.65981	5.68560	5.70708	5.72116	5.70713	5.70725	5.71839	5.70706	5.71432	5.70698
$y_\tau/10^{-2}$	0.97358	0.97054	0.97021	0.96623	0.97020	0.97211	0.97154	0.97020	0.97124	0.97020
θ_{12}^q	0.22750	0.22749	0.22739	0.22760	0.22739	0.22721	0.22745	0.22739	0.22745	0.22739
$\theta_{23}^q/10^{-2}$	4.904	4.872	4.858	4.876	4.858	4.835	4.858	4.858	4.856	4.858
$\theta_{13}^q/10^{-3}$	4.252	4.215	4.202	4.201	4.202	4.237	4.202	4.202	4.202	4.202
δ^q	1.269	1.251	1.207	1.253	1.207	1.227	1.201	1.207	1.203	1.207
$\Delta m_{21}^2/10^{-5} \text{ eV}^2$	7.53	7.50	7.50	7.50	7.50	7.48	7.50	7.50	7.50	7.50
$\Delta m_{3l}^2/10^{-3} \text{ eV}^2$	2.515	2.535	2.513	2.512	2.534	2.539	2.513	2.513	2.534	2.534
$\sin^2\theta_{12}^l$	0.313	0.309	0.309	0.303	0.309	0.308	0.309	0.309	0.309	0.309
$\sin^2\theta_{23}^l$	0.456	0.561	0.470	0.460	0.561	0.540	0.471	0.470	0.561	0.561
$\sin^2\theta_{13}^l$	0.02152	0.02180	0.02215	0.02235	0.02195	0.02223	0.02217	0.02215	0.02194	0.02195
$\chi^2/(n_{\text{obs}} = 18)$	1.54	1.71	$5.88 \cdot 10^{-6}$	0.312	$7.60 \cdot 10^{-6}$	0.958	0.495	$3.41 \cdot 10^{-7}$	0.462	$3.39 \cdot 10^{-7}$
m_l/eV	$3.34 \cdot 10^{-3}$	$5.60 \cdot 10^{-3}$	$5.29 \cdot 10^{-5}$	$7.81 \cdot 10^{-4}$	$5.41 \cdot 10^{-5}$	$1.52 \cdot 10^{-3}$	$3.82 \cdot 10^{-3}$	$5.46 \cdot 10^{-4}$	$3.44 \cdot 10^{-3}$	$1.03 \cdot 10^{-3}$
m_β/eV	$9.40 \cdot 10^{-3}$	$1.05 \cdot 10^{-2}$	$8.85 \cdot 10^{-3}$	$8.88 \cdot 10^{-3}$	$8.85 \cdot 10^{-3}$	$9.02 \cdot 10^{-3}$	$9.64 \cdot 10^{-3}$	$8.87 \cdot 10^{-3}$	$9.49 \cdot 10^{-3}$	$8.91 \cdot 10^{-3}$
$m_{\beta\beta}/\text{eV}$	$4.94 \cdot 10^{-3}$	$7.18 \cdot 10^{-3}$	$3.70 \cdot 10^{-3}$	$4.22 \cdot 10^{-3}$	$3.67 \cdot 10^{-3}$	$4.76 \cdot 10^{-3}$	$6.51 \cdot 10^{-3}$	$4.09 \cdot 10^{-3}$	$6.17 \cdot 10^{-3}$	$4.42 \cdot 10^{-3}$
$\delta/^\circ$	38.816	210.46	43.046	11.532	341.29	6.4034	186.19	14.663	189.07	351.61
M_1/GeV	$7.48 \cdot 10^9$	$2.56 \cdot 10^9$	$9.95 \cdot 10^4$	$7.36 \cdot 10^6$	$8.43 \cdot 10^4$	$7.13 \cdot 10^6$	$1.01 \cdot 10^3$	$1.37 \cdot 10^{10}$	$9.09 \cdot 10^2$	$2.71 \cdot 10^{10}$
M_2/GeV	$4.95 \cdot 10^{11}$	$2.14 \cdot 10^{11}$	$2.14 \cdot 10^{12}$	$6.96 \cdot 10^{10}$	$3.64 \cdot 10^{12}$	$9.07 \cdot 10^{10}$	$6.36 \cdot 10^{11}$	$2.57 \cdot 10^{11}$	$5.60 \cdot 10^{11}$	$5.01 \cdot 10^{11}$
M_3/GeV	$5.61 \cdot 10^{12}$	$2.48 \cdot 10^{12}$	$7.51 \cdot 10^{14}$	$2.29 \cdot 10^{13}$	$1.02 \cdot 10^{15}$	$2.97 \cdot 10^{13}$	$1.36 \cdot 10^{13}$	$9.45 \cdot 10^{12}$	$1.19 \cdot 10^{13}$	$2.09 \cdot 10^{13}$

[1] H. Fritzsch and P. Minkowski, *Annals Phys.* **93**, 193-266 (1975) doi:10.1016/0003-4916(75)90211-0
[2] M. S. Chanowitz, J. R. Ellis and M. K. Gaillard, *Nucl. Phys. B* **128**, 506-536 (1977) doi:10.1016/0550-3213(77)90057-8
[3] P. Ramond, [arXiv:hep-ph/9809459 [hep-ph]].
[4] J. A. Harvey, D. B. Reiss and P. Ramond, *Nucl. Phys. B*

199, 223-268 (1982) doi:10.1016/0550-3213(82)90346-7
[5] S. Weinberg, *Phys. Rev. Lett.* **43**, 1566-1570 (1979) doi:10.1103/PhysRevLett.43.1566
[6] F. Wilczek and A. Zee, *Phys. Rev. Lett.* **43**, 1571-1573 (1979) doi:10.1103/PhysRevLett.43.1571
[7] S. Weinberg, *Phys. Rev. D* **22**, 1694 (1980) doi:10.1103/PhysRevD.22.1694

TABLE V: Benchmark fit values and predictions in 2 models in the inverted ordering. Each benchmark is named, e.g., M2I2B1: Benchmark 1 of M2 in fitting data I2. $\Delta m_{3\ell}^2 = \Delta m_{32}^2 < 0$ and $m_l = m_3$ denote the lightest neutrino mass.

Physical Quantity	M2				M3			
	M2I1B1	M2I1B2	M2I2B1	M2I2B2	M3I1B1	M3I1B2	M3I2B1	M3I2B2
$y_u/10^{-6}$	2.79	4.03	2.77	3.49	2.56	2.54	2.56	2.54
$y_c/10^{-3}$	1.37	1.44	1.37	1.36	1.38	1.36	1.38	1.36
y_t	0.428	0.427	0.428	0.428	0.428	0.428	0.428	0.428
$y_d/10^{-6}$	6.92	6.82	6.60	8.92	5.95	8.05	5.95	7.93
$y_s/10^{-4}$	1.27	0.740	1.24	1.11	1.21	1.10	1.22	1.11
$y_b/10^{-2}$	0.572	0.570	0.570	0.567	0.571	0.570	0.571	0.570
$y_e/10^{-6}$	2.70369	2.70455	2.70332	2.70702	2.70333	2.70326	2.70337	2.70348
$y_\mu/10^{-4}$	5.71365	5.73366	5.70814	5.68800	5.70707	5.71460	5.70701	5.71393
$y_\tau/10^{-2}$	0.96303	0.97624	0.96926	0.98031	0.97013	0.97102	0.97008	0.97048
θ_{12}^q	0.22740	0.22733	0.22739	0.22735	0.22742	0.22741	0.22742	0.22740
$\theta_{23}^q/10^{-2}$	4.864	4.884	4.859	4.860	4.870	4.871	4.870	4.869
$\theta_{13}^q/10^{-3}$	4.140	4.194	4.195	4.036	4.201	4.146	4.200	4.152
δ^q	1.210	1.157	1.206	1.023	1.216	1.217	1.216	1.214
$\Delta m_{21}^2/10^{-5} \text{ eV}^2$	7.49	7.46	7.49	7.28	7.49	7.50	7.49	7.49
$\Delta m_{3\ell}^2/10^{-3} \text{ eV}^2$	-2.484	-2.483	-2.510	-2.509	-2.484	-2.484	-2.510	-2.510
$\sin^2 \theta_{12}^l$	0.308	0.306	0.308	0.357	0.308	0.308	0.308	0.308
$\sin^2 \theta_{23}^l$	0.569	0.556	0.565	0.520	0.550	0.567	0.562	0.578
$\sin^2 \theta_{13}^l$	0.02232	0.02228	0.02224	0.02241	0.02231	0.02237	0.02224	0.02230
$\chi^2/(n_{\text{obs}} = 18)$	0.205	4.31	0.00721	3.54	0.0680	0.717	0.0680	0.598
m_l/eV	$2.53 \cdot 10^{-4}$	$1.78 \cdot 10^{-2}$	$2.07 \cdot 10^{-4}$	$2.02 \cdot 10^{-2}$	$9.83 \cdot 10^{-3}$	$1.48 \cdot 10^{-2}$	$9.60 \cdot 10^{-3}$	$1.41 \cdot 10^{-2}$
m_β/eV	$4.88 \cdot 10^{-2}$	$5.19 \cdot 10^{-2}$	$4.90 \cdot 10^{-2}$	$5.31 \cdot 10^{-2}$	$4.97 \cdot 10^{-2}$	$5.10 \cdot 10^{-2}$	$5.00 \cdot 10^{-2}$	$5.10 \cdot 10^{-2}$
$m_{\beta\beta}/\text{eV}$	$4.82 \cdot 10^{-2}$	$5.05 \cdot 10^{-2}$	$4.83 \cdot 10^{-2}$	$5.19 \cdot 10^{-2}$	$4.94 \cdot 10^{-2}$	$5.00 \cdot 10^{-2}$	$4.96 \cdot 10^{-2}$	$5.00 \cdot 10^{-2}$
$\delta/^\circ$	307.27	101.18	326.05	69.966	327.06	347.86	202.42	14.403
M_1/GeV	$7.60 \cdot 10^3$	$4.73 \cdot 10^6$	$5.12 \cdot 10^3$	$1.84 \cdot 10^6$	$5.90 \cdot 10^5$	$7.09 \cdot 10^9$	$5.93 \cdot 10^5$	$7.14 \cdot 10^9$
M_2/GeV	$2.15 \cdot 10^{12}$	$1.45 \cdot 10^{10}$	$2.97 \cdot 10^{12}$	$1.67 \cdot 10^{10}$	$7.07 \cdot 10^{10}$	$8.17 \cdot 10^{10}$	$7.14 \cdot 10^{10}$	$8.39 \cdot 10^{10}$
M_3/GeV	$6.55 \cdot 10^{14}$	$4.30 \cdot 10^{12}$	$8.61 \cdot 10^{14}$	$5.22 \cdot 10^{12}$	$3.14 \cdot 10^{12}$	$6.45 \cdot 10^{12}$	$3.17 \cdot 10^{12}$	$6.53 \cdot 10^{12}$

- [8] S. Weinberg, Phys. Rev. D **26**, 287 (1982) doi:10.1103/PhysRevD.26.287
- [9] N. Sakai and T. Yanagida, Nucl. Phys. B **197**, 533 (1982) doi:10.1016/0550-3213(82)90457-6
- [10] S. Dimopoulos, S. Raby and F. Wilczek, Phys. Lett. B **112**, 133 (1982) doi:10.1016/0370-2693(82)90313-6
- [11] J. R. Ellis, D. V. Nanopoulos and S. Rudaz, Nucl. Phys. B **202**, 43-62 (1982) doi:10.1016/0550-3213(82)90220-6
- [12] P. Langacker, Phys. Rept. **72**, 185 (1981) doi:10.1016/0370-1573(81)90059-4
- [13] K. Abe *et al.* [Super-Kamiokande], Phys. Rev. D **90**, no.7, 072005 (2014) doi:10.1103/PhysRevD.90.072005 [arXiv:1408.1195 [hep-ex]].
- [14] K. Abe *et al.* [Super-Kamiokande], Phys. Rev. D **95**, no.1, 012004 (2017) doi:10.1103/PhysRevD.95.012004 [arXiv:1610.03597 [hep-ex]].
- [15] Y. Fukuda *et al.* [Super-Kamiokande], Phys. Rev. Lett. **81**, 1562-1567 (1998) doi:10.1103/PhysRevLett.81.1562 [arXiv:hep-ex/9807003 [hep-ex]].
- [16] F. An *et al.* [JUNO], J. Phys. G **43**, no.3, 030401 (2016) doi:10.1088/0954-3899/43/3/030401 [arXiv:1507.05613 [physics.ins-det]].
- [17] R. Acciarri *et al.* [DUNE], [arXiv:1512.06148 [physics.ins-det]].
- [18] K. Abe *et al.* [Hyper-Kamiokande], [arXiv:1805.04163 [physics.ins-det]].
- [19] A. Abusleme *et al.* [JUNO], [arXiv:2511.14593 [hep-ex]].
- [20] K. S. Babu and R. N. Mohapatra, Phys. Rev. Lett. **70**, 2845-2848 (1993) doi:10.1103/PhysRevLett.70.2845 [arXiv:hep-ph/9209215 [hep-ph]].
- [21] B. Bajc, A. Melfo, G. Senjanovic and F. Vissani, Phys. Rev. D **73**, 055001 (2006) doi:10.1103/PhysRevD.73.055001 [arXiv:hep-ph/0510139 [hep-ph]].
- [22] R. D. Peccei and H. R. Quinn, Phys. Rev. Lett. **38**, 1440-1443 (1977) doi:10.1103/PhysRevLett.38.1440
- [23] B. Fu, S. F. King, L. Marsili, S. Pascoli, J. Turner and Y. L. Zhou, JHEP **11**, 072 (2022) doi:10.1007/JHEP11(2022)072 [arXiv:2209.00021 [hep-ph]].
- [24] A. S. Joshipura and K. M. Patel, Phys. Rev. D **83**, 095002 (2011) doi:10.1103/PhysRevD.83.095002 [arXiv:1102.5148 [hep-ph]].
- [25] A. Dueck and W. Rodejohann, JHEP **09**, 024 (2013) doi:10.1007/JHEP09(2013)024 [arXiv:1306.4468 [hep-ph]].
- [26] V. S. Mummidi and K. M. Patel, JHEP **12**, 042 (2021) doi:10.1007/JHEP12(2021)042 [arXiv:2109.04050 [hep-ph]].
- [27] T. Ohlsson and M. Pernow, JHEP **06**, 085 (2019)

- doi:10.1007/JHEP06(2019)085 [arXiv:1903.08241 [hep-ph]].
- [28] K. S. Babu and S. Khan, *Phys. Rev. D* **92**, no.7, 075018 (2015) doi:10.1103/PhysRevD.92.075018 [arXiv:1507.06712 [hep-ph]].
- [29] G. Altarelli and D. Meloni, *JHEP* **08**, 021 (2013) doi:10.1007/JHEP08(2013)021 [arXiv:1305.1001 [hep-ph]].
- [30] K. S. Babu, B. Bajc and S. Saad, *JHEP* **02**, 136 (2017) doi:10.1007/JHEP02(2017)136 [arXiv:1612.04329 [hep-ph]].
- [31] S. Saad, *JHEP* **04**, 058 (2023) doi:10.1007/JHEP04(2023)058 [arXiv:2212.05291 [hep-ph]].
- [32] K. S. Babu, P. Di Bari, C. S. Fong and S. Saad, *JHEP* **10**, 190 (2024) doi:10.1007/JHEP10(2024)190 [arXiv:2409.03840 [hep-ph]].
- [33] K. S. Babu, C. S. Fong and S. Saad, [arXiv:2508.14969 [hep-ph]].
- [34] B. Dutta, Y. Mimura and R. N. Mohapatra, *Phys. Lett. B* **603**, 35-45 (2004) doi:10.1016/j.physletb.2004.09.076 [arXiv:hep-ph/0406262 [hep-ph]].
- [35] D. Chang, R. N. Mohapatra and M. K. Parida, *Phys. Rev. Lett.* **52**, 1072 (1984) doi:10.1103/PhysRevLett.52.1072
- [36] W. Grimus and H. Kuhbock, *Eur. Phys. J. C* **51**, 721-729 (2007) doi:10.1140/epjc/s10052-007-0324-5 [arXiv:hep-ph/0612132 [hep-ph]].
- [37] I. Esteban, M. C. Gonzalez-Garcia, M. Maltoni, I. Martinez-Soler, J. P. Pinheiro and T. Schwetz, *JHEP* **12**, 216 (2024) doi:10.1007/JHEP12(2024)216 [arXiv:2410.05380 [hep-ph]]; NuFIT 6.0 (2024), www.nu-fit.org.
- [38] S. Davidson and A. Ibarra, *Phys. Lett. B* **535**, 25-32 (2002) doi:10.1016/S0370-2693(02)01735-5 [arXiv:hep-ph/0202239 [hep-ph]].
- [39] P. Di Bari and A. Riotto, *JCAP* **04**, 037 (2011) doi:10.1088/1475-7516/2011/04/037 [arXiv:1012.2343 [hep-ph]].
- [40] K. S. Babu, B. Bajc and S. Saad, *JHEP* **10**, 135 (2018) doi:10.1007/JHEP10(2018)135 [arXiv:1805.10631 [hep-ph]].